Vascular mural cells protect the adult brain from haemorrhage but do not control the blood-brain barrier in developing zebrafish

Oguzhan F Baltaci[1,2], Andrea Usseglio Gaudi[1,2], Stefanie Dudczig[1,2], Weili Wang[3], Maria Cristina Rondon-Galeano[1,2], Ye-Wheen Lim[3], James Rae[3], Anne Lagendijk[3], Robert G Parton[3,6], Alison Farley[1,2,4], Benjamin M Hogan[1,2,5,#]

[1] Organogenesis and Cancer Program, Peter MacCallum Cancer Centre, Melbourne, VIC 3000, Australia.
[2] Sir Peter MacCallum Department of Oncology, University of Melbourne, Melbourne, VIC 3000, Australia.
[3] Institute for Molecular Bioscience, The University of Queensland, St Lucia, 4072, QLD, Australia
[4] Walter and Eliza Hall Institute of Medical Research, Melbourne, Victoria 3052, Australia.
[5] Department of Anatomy and Physiology, University of Melbourne, Melbourne, VIC 3000, Australia.
[6] Centre for Microscopy and Microanalysis, The University of Queensland, St Lucia, 4072, QLD, Australia

[#] *Author for Correspondence:*

Professor Ben Hogan
Organogenesis and Cancer Program,
Peter MacCallum Cancer Centre,
Melbourne, VIC 3000, Australia
E-mail: ben.hogan@petermac.org

The blood-brain barrier (BBB) protects the brain from circulating metabolites and plays central roles in neurological diseases. Endothelial cells (ECs) of the BBB are enwrapped by mural cells including pericytes and vascular smooth muscle cells (vSMCs) that regulate angiogenesis, vessel stability and barrier function. To explore mural cell control of the BBB, we investigated neurovascular phenotypes in zebrafish *pdgfrb* mutants that lack brain pericytes and vSMCs. As expected, mutants showed an altered cerebrovascular network with mis-patterned capillaries. Unexpectedly, mutants displayed no BBB leakage from larval through to young adult stages. This demonstrates that pericytes and vSMCs do not control BBB function in young zebrafish. Instead, we observed adult BBB disruption occurring at "hotspot" focal haemorrhages at major vessel aneurysms. ECs at leakage hotspots showed induction of caveolae on abluminal surfaces and major structural defects including basement membrane thickening and disruption. Our work suggests that capillary pericytes regulate cerebrovascular patterning in development and vSMCs of major arteries protect from haemorrhage and BBB breakdown in older zebrafish. The fact that young zebrafish can have a conserved BBB with intact barrier function in the absence of mural cells, warrants renewed interrogation of the paradigm of mural cell control of the BBB.

Neurovascular endothelial cells (ECs) have unique functional and structural properties to regulate substance exchange between blood and brain, establishing the blood-brain barrier (BBB)[1,2]. Loss of normal BBB function is associated with neuropathological states, including neurodegeneration, infection and cancer[1,2]. Mural cells are vascular support cells that include pericytes and vascular smooth muscle cells (vSMCs) and control vascular development, function and BBB permeability[3-9]. PDGFB/PDGFRβ signalling is required for the development of mural cells[3,4,10-12] and their depletion in PdgfB or Pdgfrβ deficient rodents causes altered angiogenesis, aneurysm and vessel leakiness[3-6,13]. Strikingly, rodent models of pericyte loss have an open BBB, with free transport of tracer dyes from the blood stream into the brain parenchyma but an otherwise intact vasculature[5,6]. These and other observations, have led to a current model whereby pericytes control BBB function by suppressing EC adsorptive transcytosis. This prominent mechanism holds significant translational promise to safely open up the BBB in therapeutic settings, by discovering ways to disrupt pericyte control of ECs[5,14].

Zebrafish have a highly conserved BBB[15-19] with the brain endothelium expressing conserved molecular markers of a functional BBB[18] and showing conserved cellular interactions with pericytes, smooth muscle cells and glial cells[20,21]. The zebrafish BBB becomes functional by 5 days post fertilisation (dpf)[19] and as in mice, *pdgfrb* mutants lack brain pericytes and exhibit loss of vSMCs[13,20]. Thus, the zebrafish is accepted as a highly accessible model to study BBB

83 function and mural cell control of the BBB[17]. To investigate the influence of mural cells upon
84 the neurovasculature, we generated a *pdgfrb* mutant (*pdgfrb*^{uq30bh}), which possesses an early
85 deletion leading to a frameshift, predicted to cause a premature stop codon and a putative null
86 allele. Using the *TgBAC(pdgfrb:egfp)*^{ncv22} line, we observed that pericytes were lost in the
87 cerebral central arteries of *pdgfrb* mutants (**Fig. 1a**), as in previous studies[13,20]. To assess how
88 brain angiogenesis occurs without pericytes, we imaged, traced and quantified blood vessel
89 branching from the middle mesencephalic central arteries in the midbrain **(Fig. 1a-c;**
90 **Extended Data Fig. 1a)**. At 7 dpf, mutants displayed significantly reduced vascular complexity
91 compared to siblings, with reduced vessel length and branch points **(Fig. 1d-e)**. This was more
92 severe at 14 dpf, demonstrating the phenotype is progressive **(Fig. 1d-e)**. Timecourse imaging
93 revealed the reduction in vascular complexity was apparent from 5 dpf (**Extended Data Fig.**
94 **1a-b)**. These results suggest that pericytes (the vSMCs only begin to develop after 5 dpf[22])
95 regulate angiogenesis from early in larval development.
96
97 We next tested BBB function in mutants at 7 and 14 dpf. We performed intravenous injection
98 of fluorescently conjugated tracers of various molecular weights (1 kDa NHS, 10 kDa and 70
99 kDa Dextran), and live imaged fish at 2 hours after injection (as in [19]) **(Fig. 1f; Extended Data**
100 **Fig, 1c)**. 2000 kDa Dextran was coinjected to normalize quantification of vascular tracer dye
101 delivery (see methods for details). We found no evidence of 10 kDa or 70 kDa Dextran tracer
102 extravasation into the brain parenchyma of *pdgfrb*^{uq30bh} mutants at either timepoint **(Fig. 1g;**
103 **Extended Data Fig. 1c-e)**. 1 kDa tracer showed no difference between genotypes but was
104 observable in the parenchyma in both sibling and mutants, indicating the smaller cargo can
105 pass the BBB (**Extended Data Fig. 1c & e)**. Together, these results show that neither pericytes
106 nor vSMCs play a role in establishment of BBB function in larval zebrafish.
107
108 To investigate how mural cells control cerebral vasculature at later stages of life, we tissue-
109 cleared brains of adult stage *pdgfrb*^{uq30bh} mutants and siblings[23] and performed whole brain
110 imaging. We confirmed loss of pericytes and vSMCs at this stage **(Fig. 2a)**. We examined a
111 consistent region of the left optic tectum (mid brain) and detected decreased branching of
112 capillaries and increased diameter of major vessels **(Fig. 1b-d)**. This vessel dilation was
113 restricted to larger calibre arteries that would normally be invested with vSMCs and not seen
114 in capillaries **(Fig. 1c-d)**. This suggests vessel dilation in mutants is due to loss of vSMCs and
115 reduced branching of capillaries to loss of pericytes.
116
117 We assessed BBB function in juvenile 2-month-old zebrafish by intravenous tracer injection
118 (as in [24]) and using a mixture of 70- and 2000 kDa Dextran. We euthanized fish 2 hours post-
119 injection and tissue-cleared the brains. The whole brain imaging revealed that mutants

120 displayed widespread aneurysm of major vessels **(Fig. 2e-f, Extended Data Fig. 2a-a´)**. To
121 quantify potential BBB leakage, we imaged a consistent region with high capillary density **(Fig.**
122 **2e´)**, and quantified parenchymal 70 kDa Dextran intensity relative to vascular 2000 kDa
123 Dextran intensity. Both tracers remained restricted to the vascular lumen regardless of the
124 severity of the aneurysms **(Fig. 2g)**. This correlates with our findings at larval stages and
125 demonstrated that mural cells are dispensable for the establishment and early maturation of
126 the BBB in zebrafish up to 2 months of age.
127
128 To investigate BBB integrity at later stages, we injected 3-month-old adult zebrafish with 10 or
129 70 kDa Dextran. Brightfield imaging of vibratome sectioned brains revealed severe aneurysms
130 across large calibre vessels **(Fig. 3a)** with blood pooling that was potentially consistent with
131 vessel ruptures **(Fig. 3c)**. Furthermore, we detected parenchymal accumulation of tracer dye
132 closely associated with large calibre vessel aneurysms **(Fig. 3b-c; Extended Data Fig. 3a-**
133 **a´)**. To quantify the distribution of parenchymal tracer dye from deep (around major artery
134 aneurysms) to superficial (in capillary beds) brain regions, we measured fluorescence intensity
135 in 10 brain regions 100 microns apart from medial to lateral locations. This demonstrated
136 accumulation of tracer dye in medial regions associated with aneurysm in mutants, with no
137 evidence of major leakage in capillary beds **(Fig. 3d-e)**. To better understand the extravasated
138 tracer accumulation, we conducted whole brain imaging after 70 kDa Dextran injection.
139 Interestingly, we observed highly localised tracer accumulated in regions that could be
140 considered leakage "hotspots" at large calibre vessel aneurysms **(Fig. 4a; Extended Data**
141 **Fig. 4a; Supplementary Videos 1 and 2)**. Quantification of three independent whole cleared
142 brains throughout the optic tecta revealed on average 11 hotspots occurring at major vessels
143 in each mutant animal **(Fig. 4b)**. To further understand the nature of these hotspots, we
144 examined red blood cells in *pdgfrb* mutant adults (Crispants, validated in **Extended Data Fig.**
145 **4b**) using the *Tg(gata1:DsRed)*^{sd2} transgenic line together with tracer injection. These animals
146 showed that tracer accumulation occurred concomitant with extravasated red blood cells at
147 hotspots, identifying them as focal haemorrhages **(Fig. 4c)**. Notably, these sites were not
148 detected at capillaries **(Fig. 4d)**. Taken together, this shows that in older mutants, loss of BBB
149 integrity is associated with focal haemorrhage along aneurysmal vessels.
150
151 Pericytes are proposed to regulate the BBB by suppressing adsorptive transcytosis through
152 brain capillary ECs[5,6]. This model is built on the observation by electron microscopy of the
153 induction of caveolae in leaky pericyte deficient vessels[5,6]. To investigate if the loss of BBB
154 integrity is associated with ultrastructural changes, we performed electron microscopy. We
155 imaged large calibre vessels and capillaries **(Fig. 4e; Extended Data Fig. 4c)** and examined
156 cellular junctions, basement membrane and caveolae (defined as uncoated vesicular profiles

157 of <100nm diameter). While tight junctions between endothelial cells remained intact (**Fig. 4f**),
158 Caveola density along the large vessel aneurysms in *pdgfrb*^{uq30bh} mutants was significantly
159 increased. This increase was almost exclusive to the abluminal side of the ECs **(Fig. 4g).** This
160 abluminal accumulation of caveolae may be more associated with changes in the mechanical
161 state of ECs (as caveolae are highly regulated by membrane tension[25,26]) than changes in
162 intracellular transport. Furthermore, we detected thickening of basement membrane (BM) (**Fig.**
163 **4g**), gaps in the BM and fluid accumulation outside the vessel wall at aneurysms in mutants.
164 We found no obvious difference in the caveolae density of capillary ECs of *pdgfrb*^{uq30bh} mutants
165 compared with siblings **(Extended Data Fig. 4d)**. Thus, leakage hotspots at aneurysms are
166 associated with a failure of the normal flattening of ECs, caveola induction and disruption of
167 the BM, all factors that could contribute to or be observed concurrent with vessel wall rupture.
168
169 Brain vasculature is endowed with mural cells that control vascular development and
170 stability[3,4,13,27]. Studies in rodents have shown that pericytes regulate BBB integrity[5,6]. This is
171 currently thought to be caused by hotspots of increased EC transcytosis[14], rather than
172 mechanisms such as altered cell-cell adhesion (eg, Cldn5[14]), control of Mfsd2a[19,28], Netrin1-
173 Unc5B signalling[29] or vitronectin regulation of integrin receptors[30]. However, some studies in
174 rodents have reported loss of pericytes without vessel leakage[31]. We show mural cells are
175 involved in cerebrovascular patterning in larval, juvenile and young adult animals but these
176 vessels maintain BBB function in the absence of mural cells. In our mutants, major arteries
177 progressively harbour aneurysms. This aneurysm is likely associated with loss of vSMCs[13].
178 At later stages, adult mutants show leakage at hotspots distributed along aneurysms, which
179 are focal haemorrhages. In some PDGFB/PDGFRβ mouse mutants, haemorrhages have
180 been reported, but not in mild or hypomorphic mutants such as those used in BBB studies[3,4,12].
181 In our model, BBB leakage appears to only be observed once haemorrhage is present. Of
182 course, these observations could represent a species-specific divergence from the
183 mammalian BBB. However, the zebrafish BBB appears highly conserved with that of
184 mammals[17] and we would argue that the importance of BBB function for vertebrate brain
185 physiology throughout evolution makes divergence unlikely. We suggest that a deeper
186 analysis of the nature of hotspot leakage in mural cell deficient mammalian models is
187 warranted. Altogether, a deeper understanding of the fundamental biology of the BBB will pave
188 the way for increasingly sophisticated efforts to target the BBB in disease in the future.
189

190 **Acknowledgments**

191 This project was supported in part by funding from Bright focus (A2018807S) and the
192 Australian Research Council (ARC) (DP210102712) and The Brain Cancer Centre (founded

by Carrie's Beanies for Brain Cancer). B.M.H was supported by a National Health and Medical Research Council Senior Research Fellowship (1155221). O.F.B was supported by the Brain Cancer Centre Blood-Brain Barrier Program. R.G.P was supported by an ARC Laureate Fellowship (FL210100107). We thank the Centre for Advanced Histology and Microscopy (RRID:SCR_025432) at the Peter MacCallum Cancer Centre and Microscopy Australia Research Facility at the Centre for Microscopy and Microanalysis at The University of Queensland. We also thank Kelly Smith and Marcos Sande Melon for academic discussions and technical suggestions.

Author contributions

O.B performed, analysed experiments and co-wrote manuscript. B.M.H, conceptualised experiments, analysed data and co-wrote manuscript. A.U.G, S.D, W.W, M.C.R.G, Y.W.L, J.R, R.P, A.L and A.F performed and analysed experiments.

Conflicts of interest

The authors declare no conflict of interests.

Fig. 1: Pericyte-deficient larval brain vasculature displays abnormal patterning but an intact blood-brain barrier

a, Confocal projections of pericytes (*TgBAC(pdgfrb:egfp)*^{ncv22}) and brain vasculature (*Tg(kdrl:Hsa.HRAS-mCherry)*^{s843}) in sibling and *pdgfrb*^{uq30bh} mutants at 7 dpf.
a′, Zoomed section from **a** (dashed rectangle) showing the midbrain central arteries.

b, Midbrain central arteries in sibling and *pdgfrb*^{uq30bh} mutants at 14 dpf.

c, Representative images of vascular tracing at 7 dpf using Imaris 10.1 software. Lumenized blood vessels branching from the middle mesencephalic central arteries in the midbrain were traced.

d,e, Quantification of midbrain vessel length (**d**) and branching points (**e**). N=8 per group, unpaired *t*-test, **P*<0.05, ***P*<0.01.

f, Fluorescent tracer assays in the midbrain of zebrafish larvae. 10 kDa Dextran–Cascade Blue and 70 kDa Dextran–Fluorescein were used to detect tracer extravasation to the brain parenchyma (white squares) in separate experiments and were coinjected with 2000 kDa Dextran–Tetramethylrhodamine to normalize vascular tracer intensity. Representative image of 2000 kDa Dextran was taken from 70 kDa Dextran coinjection, and 10 kDa Dextran coinjection is shown in Extended Data Fig. 1.

g, Quantification of brain parenchymal 70 kDa and 10 kDa Dextran intensity normalized to the vascular 2000 kDa Dextran intensity. N=15 in sibling and n=7 in *pdgfrb*^{uq30bh} for 70 kDa Dextran intensity, n=8 in sibling, n=9 in *pdgfrb*^{uq30bh} for 10 kDa Dextran intensity. Unpaired *t*-test, ns=not significant.

a,**a′, b, c, f,** Scale bars: 100 μm.

Extended Data Fig. 1: *pdgfrb*^{uq30bh} larvae exhibit decreased cerebrovascular complexity but an intact BBB.

a, Confocal projections of pericytes (*TgBAC(pdgfrb:egfp)*^{ncv22}) and brain vasculature (*Tg(kdrl:Hsa.HRAS-mCherry)*^{s843}) in sibling and *pdgfrb*^{uq30bh} mutants at 3-5 dpf.

b, Quantification of branching points of midbrain central arteries demonstrating the first detectable vessel patterning phenotype is seen at 5 dpf. N=10 per group at 3 dpf, n=15 in sibling and n=9 in *pdgfrb*^{uq30bh} at 4 dpf, n=15 in sibling and n=11 in *pdgfrb*^{uq30bh} at 5 dpf. Unpaired *t*-test, ns=not significant, *$P<0.05$.

c, d, Fluorescent tracer leakage assays in the midbrain of zebrafish larvae at 7 (**c**) and 14 dpf (**d**). 70 kDa Dextran–Fluorescein, 10 kDa Dextran–Cascade Blue and 1 kDa NHS Ester–Alexa Fluor 405 were used to detect tracer extravasation to the brain parenchyma in separate experiments and were coinjected with 2000 kDa Dextran–Tetramethylrhodamine to normalize vascular tracer intensity.

e, Quantification of brain parenchymal 70- and 10- and 1 kDa tracer intensity normalized to vascular 2000 kDa Dextran intensity. N=12 for sibling and n=7 in *pdgfrb*^{uq30bh} 1 kDa NHS Ester intensity at 7 dpf, n=10 in sibling and n=9 in *pdgfrb*^{uq30bh} for 70 kDa intensity at 14dpf, n=6 for sibling and n=4 for *pdgfrb*^{uq30bh} for 10 kDa intensity at 14 dpf. Unpaired *t*-test, ns=not significant.

a, c, d, Scale bars: 100 μm.

Fig. 2: *pdgfrb*^{uq30bh} mutants develop aneurysms but display an intact blood-brain barrier at 2 months of age.

a, Confocal projections of whole brain imaging showing mural cells (*TgBAC(pdgfrb:egfp)*^{ncv22}) and brain vasculature (*Tg(kdrl:Hsa.HRAS-mCherry)*^{s843}) in sibling and *pdgfrb*^{uq30bh} mutants at 5-months of age.

b, Restricted regions from the whole brain imaging in **a** (approximate location of dotted line) indicating pericyte loss and abnormal capillary network patterning. 100-µm thick maximum intensity projections (MIP) were generated using the continuation of the left middle mesencephalic central artery (arrow) as an anatomical anchor point.

c, d, Quantification of capillary branching points, large vessel and capillary diameter using the area shown in **b**. Large vessel diameter was quantified by averaging 5 points per vessel and the capillary diameter was quantified by averaging 10 capillary diameter per sample. N=3 per group, unpaired *t*-test, $^{**}P<0.01$, ns=not significant.

e, Fluorescent tracer assays in the midbrain of 2-month-old zebrafish. 70 kDa Dextran–Fluorescein and 2000 kDa Dextran–Tetramethylrhodamine were co-injected to detect the tracer extravasation to the brain parenchyma and the tracer within the vasculature, respectively. Arrowheads indicate examples of aneurysms.
e′, Confocal projections zoomed in on the approximate area shown in **e** (dashed rectangle). 30-µm thick MIPs were generated to examine the capillary leakage, starting 30 µm below the most superficial point of the left hemisphere of the brain to prevent the potential leakage from the superficial vessels.

f, Quantification of the severity of aneurysms in sibling (n=11) or *pdgfrb*^{uq30bh} (n=11). For examples of "severe" and "mild" see Extended Data Fig. 2.

g, Quantification of the brain parenchymal 70 kDa Dextran intensity normalized to the vascular 2000 kDa Dextran intensity, n=5 in sibling, n=4 in *pdgfrb*^{uq30bh} mutants, unpaired *t*-test, ns=not significant.

a, b, e, e′, Scale bars: 250 µm.

298 **Extended Data Fig. 2: Examples of aneurysms in *pdgfrb*^{uq30bh} mutants at 2-month-old**
299 **stage.**
300
301 **a**, Fluorescent tracer assays in the midbrain of 2-month-old zebrafish displaying examples of
302 aneurysm severity in major vessels. 70 kDa Dextran–Fluorescein and 2000 kDa Dextran–
303 Tetramethylrhodamine were co-injected to detect tracer extravasation to the brain parenchyma
304 and tracer within the vasculature, respectively.
305 **a′,** Confocal projections zoomed in on the area shown in **a** (dashed square). Aneurysm
306 (arrowheads) phenotypes were qualitatively categorised based on severity; normal, mild and
307 severe and these categories used in Fig. 2.

Fig. 3: Adult *pdgfrb*^{uq30bh} mutants display aneurysms and vascular integrity defects.

a, Representative images of coronal midbrain sections obtained from 3 month-old sibling and *pdgfrb*^{uq30bh} animals.

b, Fluorescent tracer assays in 3-month-old sibling and *pdgfrb*^{uq30bh} mutant animals. 10 kDa Dextran–Cascade Blue (cyan) was retro-orbitally injected, and *Tg(kdrl:Hsa.HRAS-mCherry)*^{s843} was used to label the blood vessels (magenta). Scale bar: 250 μm.

c, Zoomed regions from **a** and **b** (dotted squares) displaying blood and tracer accumulation (arrows).

d, Zoomed regions from **b** (dashed rectangle) displaying vasculature and tracer dye leakage from medial (large vessel) to lateral (capillary region) locations. The area was divided into 10 regions every 100 μm for tracer leakage quantification.

e, Quantification of brain parenchymal dextran intensity at medial (large vessel) to lateral (capillary region) locations shown in **d**. N=5 in sibling, n=4 in *pdgfrb*^{uq30bh}, Two-sample Kolmogorov-Smirnov test, error bars represent SEM.

329
330 **Extended Data Fig. 3: Adult *pdgfrb*^{uq30bh} mutant animals display leakage and tracer**
331 **accumulation localised at major vessel aneurysms.**
332
333 **a,** Fluorescent tracer leakage assays in 5-month-old sibling and *pdgfrb*^{uq30bh} animals. 70 kDa
334 Dextran–Fluorescein (green) was retro-orbitally injected, and *Tg(kdrl:Hsa.HRAS-mCherry)*^{s843}
335 was used to label the blood vessels (magenta). Scale bar: 250 μm.
336
337 **a′,** Zoomed regions (dashed rectangles) from **a** highlighting the tracer accumulation outside
338 the large calibre vessels with aneurysm. Scale bar: 250 μm.
339

Fig. 4: Adult *pdgfrb* mutants display structural endothelial cell defects, vessel rupture and tracer accumulation at aneurysm hotspots.

a, Sections from whole brain imaging showing brain vasculature (*Tg(kdrl:Hsa.HRAS-mCherry)*^{s843}) and 70 kDa Dextran Fluorescein at 5-months of age. Inset images within dashed rectangle show areas of hot spot leakage sites (arrows).

b, Quantification of hotspot leakage sites per animal in the midbrain region. N=3 for each group, unpaired *t*-test, ***P<0.01.

c, d, High resolution imaging of large calibre vessels and capillary zones in brain regions of *pdgfrb* crispants and uninjected siblings at 10-week-old stage. 10 kDa Dextran–Cascade Blue (cyan) injected, blood vessels (*Tg(kdrl:EGFP)*^{s843}) and red blood cells (*Tg(gata1:DsRed)*^{sd2}) are shown in MIPs and single Z-sections **(c).** Hotspot leakage sites are indicated by arrows. Capillary zones are shown in MIPs for all three channels and the single 10 kDa Dextran channel showing a lack of hotspot leakage site **(d)**.

e, Transmission electron microscopy images of sectioned adult zebrafish brain vessels. *pdgfrb*^{uq30bh} mutants showed basement membrane thickening and breakdown (cyan, black arrow), serum accumulation outside the vessels (white arrow), increased abluminal endothelial caveolae (magenta). Pseudo colours shown are ECs (purple), basement membrane (cyan), caveolae (magenta) and vesicles larger than 100 nm (green). Scale bars: 2 µm.

f, Zoomed regions from **(e)** showing intact tight junctions (arrowheads) in both siblings and *pdgfrb*^{uq30bh} mutants. Scale bar: 1 µm.

g, Quantification of endothelial caveolae and basement membrane thickness. Caveolae were defined as uncoated spherical profiles <100 nm in diameter and scored as luminal or abluminal (see methods). Measurements were made for n=3 vessels for each group and a total of 8 different cellular regions measured for siblings and 19 for mutants. Basement membrane thickness was scored in 6 different regions per vessel with n=8 vessels in siblings and n=4 vessels in *pdgfrb*^{uq30bh} mutants. Unpaired *t*-test, ***P<0.001, ****P<0.0001, ns= not significant.

Extended Data Fig. 4: Adult *pdgfrb* mutant rupture hotspots at aneurysms and unchanged endothelial ultrastructure in capillaries.

a, Whole brain imaging showing midbrain vasculature (*Tg(kdrl:Hsa.HRAS-mCherry)*^{s843}) and 70 kDa Dextran–Fluorescein (green) in siblings and *pdgfrb*^{uq30bh} mutants at 5-months of age. Hotspot leakage sites are indicated by white arrowheads.

b, Confocal projections of pericytes (*TgBAC(pdgfrb:egfp)*^{ncv22}) and brain vasculature (*Tg(kdrl:Hsa.HRAS-mCherry)*^{s843}) in sibling and *pdgfrb* crispants at 5 dpf, showing loss of pericytes in the *pdgfrb* crispants (phenocopying null mutants).

c, Quantification of endothelial caveolae in capillaries of siblings and *pdgfrb*^{uq30bh} mutants. n=5 vessels per group, unpaired *t*-test ns= not significant.

387

388 **References**

389 1 Zhao, Z., Nelson, A. R., Betsholtz, C. & Zlokovic, B. V. Establishment and
390 Dysfunction of the Blood-Brain Barrier. *Cell* **163**, 1064-1078 (2015).
391 https://doi.org:10.1016/j.cell.2015.10.067
392 2 Armulik, A., Genove, G. & Betsholtz, C. Pericytes: developmental, physiological,
393 and pathological perspectives, problems, and promises. *Dev Cell* **21**, 193-215
394 (2011). https://doi.org:10.1016/j.devcel.2011.07.001
395 3 Leveen, P. *et al.* Mice deficient for PDGF B show renal, cardiovascular, and
396 hematological abnormalities. *Genes Dev* **8**, 1875-1887 (1994).
397 https://doi.org:10.1101/gad.8.16.1875
398 4 Lindahl, P., Johansson, B. R., Leveen, P. & Betsholtz, C. Pericyte loss and
399 microaneurysm formation in PDGF-B-deficient mice. *Science* **277**, 242-245
400 (1997). https://doi.org:10.1126/science.277.5323.242
401 5 Armulik, A. *et al.* Pericytes regulate the blood-brain barrier. *Nature* **468**, 557-
402 561 (2010). https://doi.org:10.1038/nature09522
403 6 Daneman, R., Zhou, L., Kebede, A. A. & Barres, B. A. Pericytes are required for
404 blood-brain barrier integrity during embryogenesis. *Nature* **468**, 562-566 (2010).
405 https://doi.org:10.1038/nature09513
406 7 Eilken, H. M. *et al.* Pericytes regulate VEGF-induced endothelial sprouting
407 through VEGFR1. *Nat Commun* **8**, 1574 (2017).
408 https://doi.org:10.1038/s41467-017-01738-3
409 8 Simonavicius, N. *et al.* Pericytes promote selective vessel regression to
410 regulate vascular patterning. *Blood* **120**, 1516-1527 (2012).
411 https://doi.org:10.1182/blood-2011-01-332338
412 9 Benjamin, L. E., Hemo, I. & Keshet, E. A plasticity window for blood vessel
413 remodelling is defined by pericyte coverage of the preformed endothelial
414 network and is regulated by PDGF-B and VEGF. *Development* **125**, 1591-1598
415 (1998). https://doi.org:10.1242/dev.125.9.1591
416 10 Hellstrom, M., Kalen, M., Lindahl, P., Abramsson, A. & Betsholtz, C. Role of
417 PDGF-B and PDGFR-beta in recruitment of vascular smooth muscle cells and
418 pericytes during embryonic blood vessel formation in the mouse. *Development*
419 **126**, 3047-3055 (1999). https://doi.org:10.1242/dev.126.14.3047
420 11 Hirschi, K. K., Rohovsky, S. A. & D'Amore, P. A. PDGF, TGF-beta, and
421 heterotypic cell-cell interactions mediate endothelial cell-induced recruitment of
422 10T1/2 cells and their differentiation to a smooth muscle fate. *J Cell Biol* **141**,
423 805-814 (1998). https://doi.org:10.1083/jcb.141.3.805
424 12 Soriano, P. Abnormal kidney development and hematological disorders in
425 PDGF beta-receptor mutant mice. *Genes Dev* **8**, 1888-1896 (1994).
426 https://doi.org:10.1101/gad.8.16.1888
427 13 Ando, K. *et al.* Conserved and context-dependent roles for pdgfrb signaling
428 during zebrafish vascular mural cell development. *Dev Biol* **479**, 11-22 (2021).
429 https://doi.org:10.1016/j.ydbio.2021.06.010
430 14 Mae, M. A. *et al.* Single-Cell Analysis of Blood-Brain Barrier Response to
431 Pericyte Loss. *Circ Res* **128**, e46-e62 (2021).
432 https://doi.org:10.1161/CIRCRESAHA.120.317473
433 15 Jeong, J. Y. *et al.* Functional and developmental analysis of the blood-brain
434 barrier in zebrafish. *Brain Res Bull* **75**, 619-628 (2008).
435 https://doi.org:10.1016/j.brainresbull.2007.10.043

16 Xie, J., Farage, E., Sugimoto, M. & Anand-Apte, B. A novel transgenic zebrafish model for blood-brain and blood-retinal barrier development. *BMC Dev Biol* **10**, 76 (2010). https://doi.org:10.1186/1471-213X-10-76

17 Quinonez-Silvero, C., Hubner, K. & Herzog, W. Development of the brain vasculature and the blood-brain barrier in zebrafish. *Dev Biol* **457**, 181-190 (2020). https://doi.org:10.1016/j.ydbio.2019.03.005

18 Umans, R. A. *et al.* CNS angiogenesis and barriergenesis occur simultaneously. *Dev Biol* **425**, 101-108 (2017). https://doi.org:10.1016/j.ydbio.2017.03.017

19 O'Brown, N. M., Megason, S. G. & Gu, C. Suppression of transcytosis regulates zebrafish blood-brain barrier function. *Elife* **8** (2019). https://doi.org:10.7554/eLife.47326

20 Ando, K. *et al.* Clarification of mural cell coverage of vascular endothelial cells by live imaging of zebrafish. *Development* **143**, 1328-1339 (2016). https://doi.org:10.1242/dev.132654

21 Chen, J., Poskanzer, K. E., Freeman, M. R. & Monk, K. R. Live-imaging of astrocyte morphogenesis and function in zebrafish neural circuits. *Nat Neurosci* **23**, 1297-1306 (2020). https://doi.org:10.1038/s41593-020-0703-x

22 Ando, K. *et al.* Peri-arterial specification of vascular mural cells from naive mesenchyme requires Notch signaling. *Development* **146** (2019). https://doi.org:10.1242/dev.165589

23 Matsumoto, K. *et al.* Advanced CUBIC tissue clearing for whole-organ cell profiling. *Nat Protoc* **14**, 3506-3537 (2019). https://doi.org:10.1038/s41596-019-0240-9

24 Pugach, E. K., Li, P., White, R. & Zon, L. Retro-orbital injection in adult zebrafish. *J Vis Exp* (2009). https://doi.org:10.3791/1645

25 Sinha, B. *et al.* Cells respond to mechanical stress by rapid disassembly of caveolae. *Cell* **144**, 402-413 (2011). https://doi.org:10.1016/j.cell.2010.12.031

26 Del Pozo, M. A., Lolo, F. N. & Echarri, A. Caveolae: Mechanosensing and mechanotransduction devices linking membrane trafficking to mechanoadaptation. *Curr Opin Cell Biol* **68**, 113-123 (2021). https://doi.org:10.1016/j.ceb.2020.10.008

27 Rajan, A. M., Ma, R. C., Kocha, K. M., Zhang, D. J. & Huang, P. Dual function of perivascular fibroblasts in vascular stabilization in zebrafish. *PLoS Genet* **16**, e1008800 (2020). https://doi.org:10.1371/journal.pgen.1008800

28 Andreone, B. J. *et al.* Blood-Brain Barrier Permeability Is Regulated by Lipid Transport-Dependent Suppression of Caveolae-Mediated Transcytosis. *Neuron* **94**, 581-594 e585 (2017). https://doi.org:10.1016/j.neuron.2017.03.043

29 Boye, K. *et al.* Endothelial Unc5B controls blood-brain barrier integrity. *Nat Commun* **13**, 1169 (2022). https://doi.org:10.1038/s41467-022-28785-9

30 Ayloo, S. *et al.* Pericyte-to-endothelial cell signaling via vitronectin-integrin regulates blood-CNS barrier. *Neuron* **110**, 1641-1655 e1646 (2022). https://doi.org:10.1016/j.neuron.2022.02.017

31 Park, D. Y. *et al.* Plastic roles of pericytes in the blood-retinal barrier. *Nat Commun* **8**, 15296 (2017). https://doi.org:10.1038/ncomms15296

Figure 1

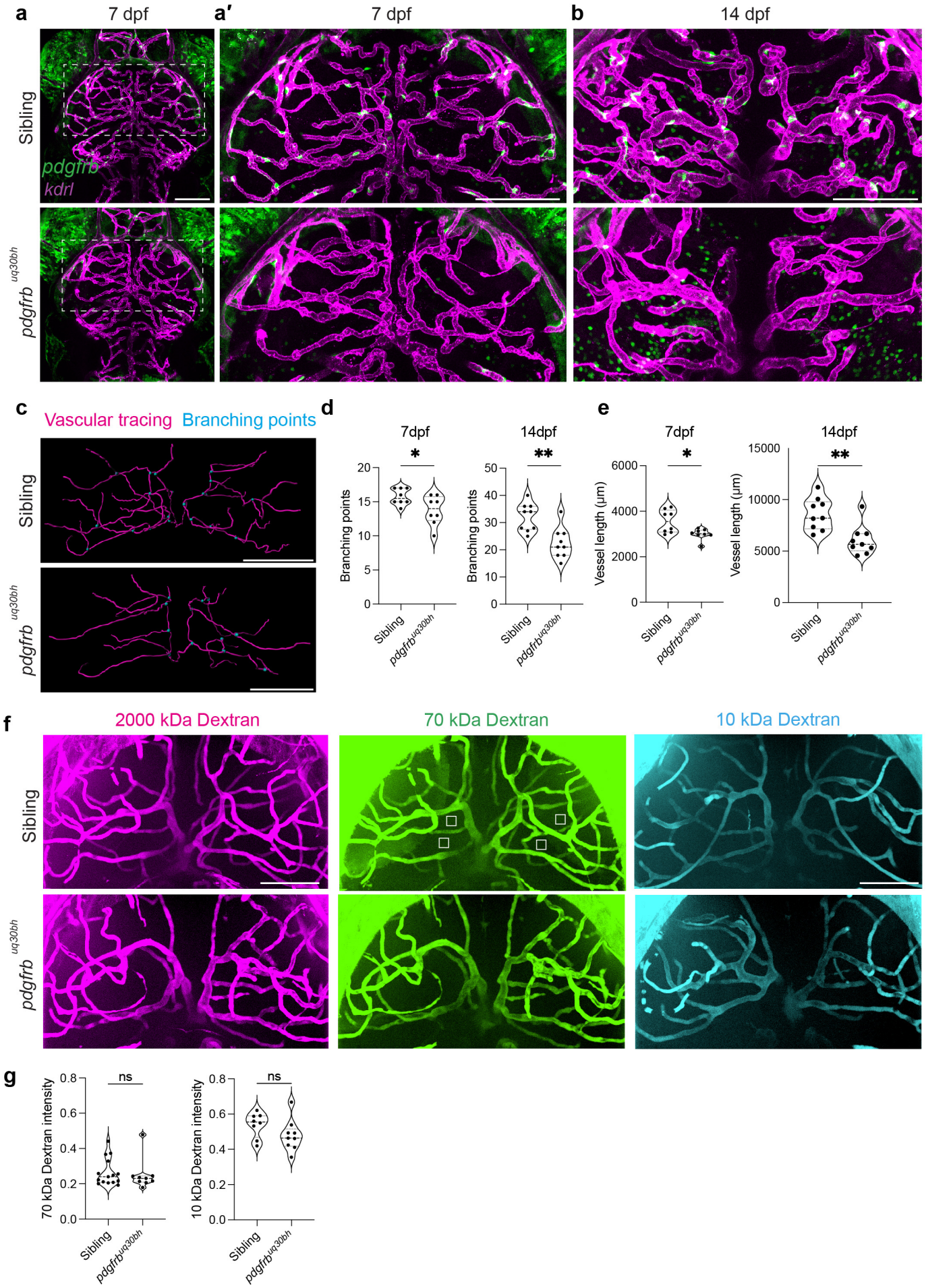
a
7 dpf
a′
7 dpf
b
14 dpf
Sibling
pdgfrb
kdrl
uq30bh
pdgfrb
c
Vascular tracing
Branching points
Sibling
uq30bh
pdgfrb
d
7dpf
14dpf
Branching points
*
**
Sibling
pdgfrb uq30bh
e
7dpf
14dpf
Vessel length (µm)
*
**
Sibling
pdgfrb uq30bh
f
2000 kDa Dextran
70 kDa Dextran
10 kDa Dextran
Sibling
uq30bh
pdgfrb
g
70 kDa Dextran intensity
10 kDa Dextran intensity
ns
ns
Sibling
pdgfrb uq30bh

Extended Data Figure 1

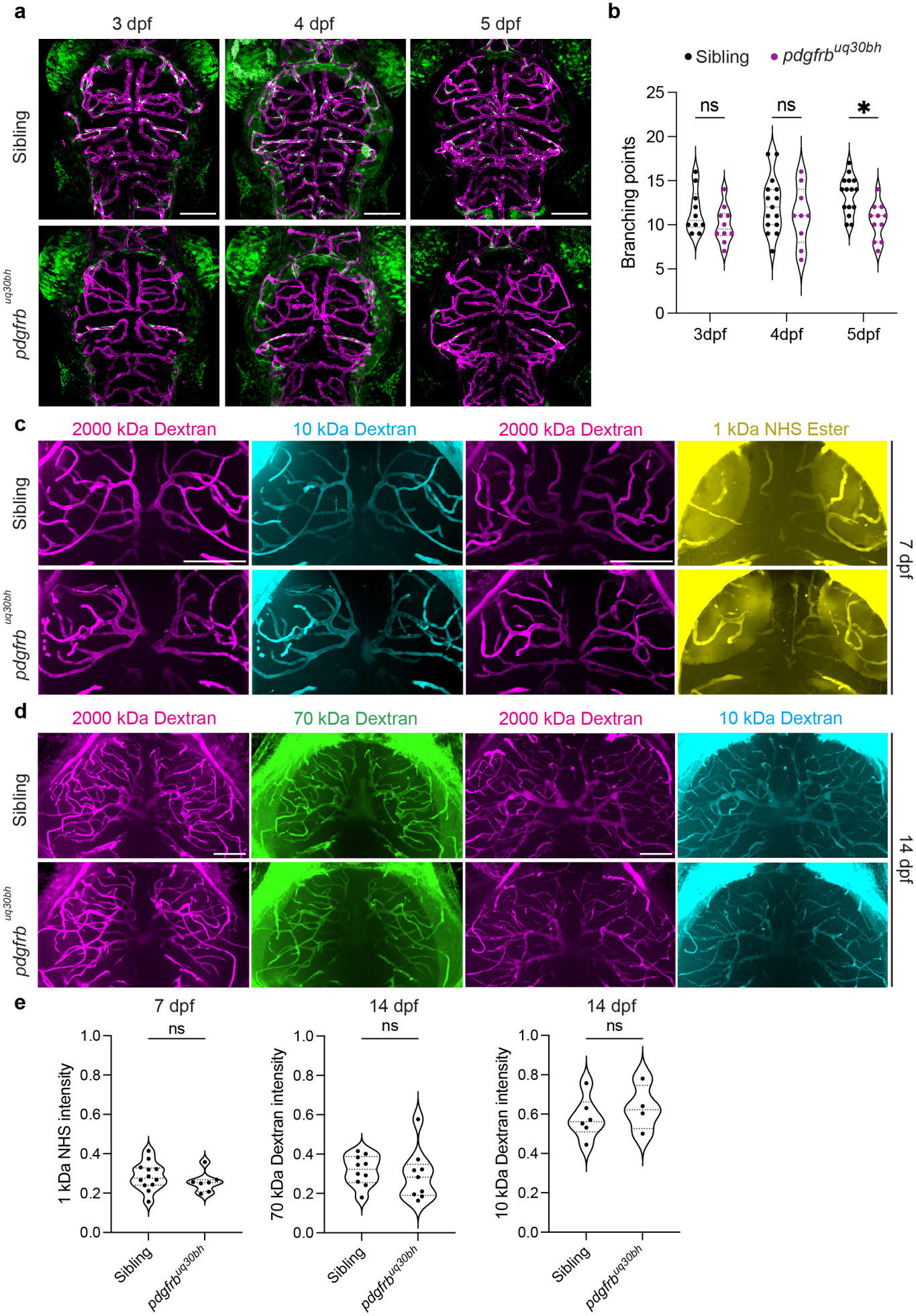

Figure 2

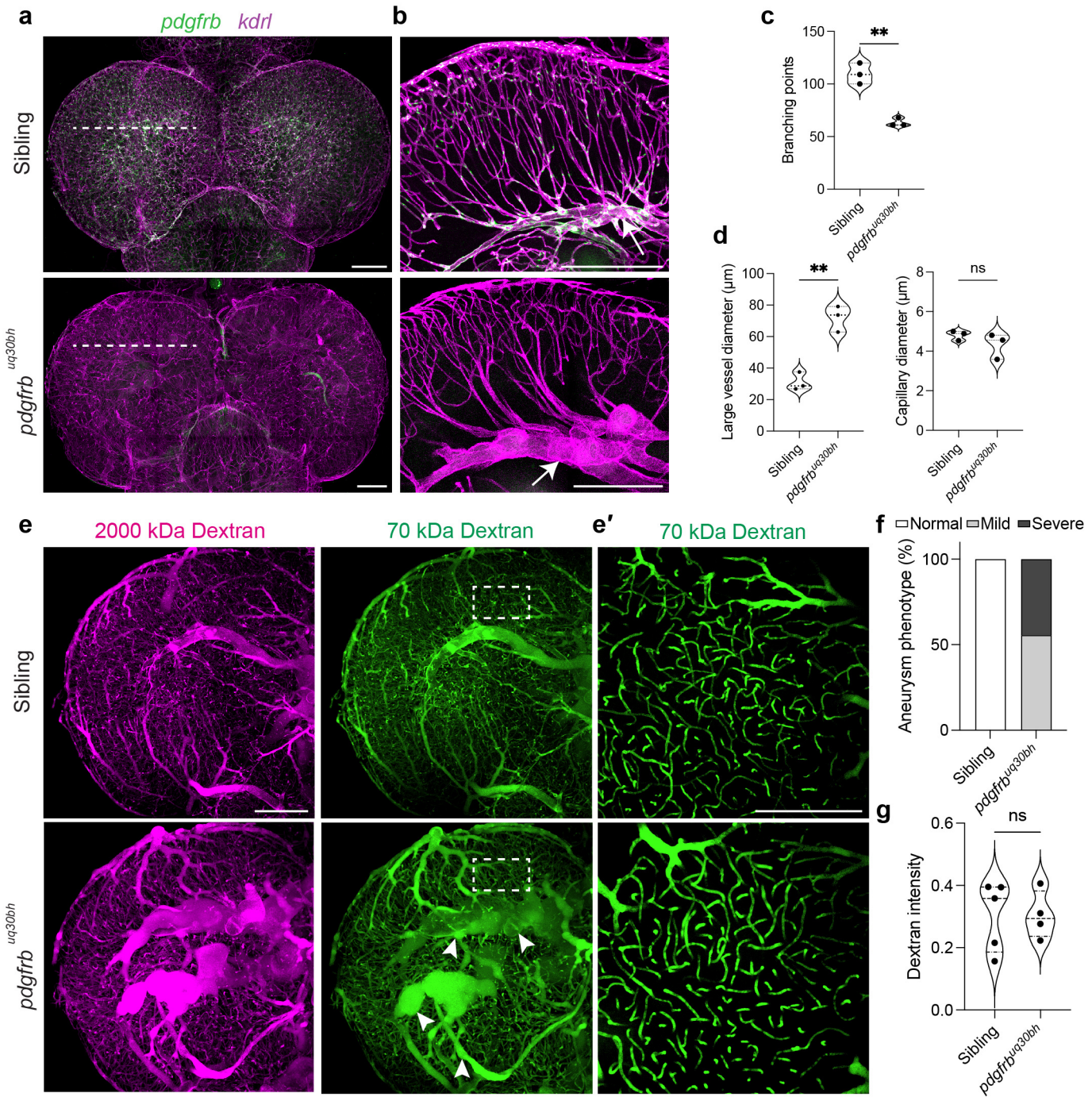
a
pdgfrb kdrl
b
Sibling
pdgfrb uq30bh
c
Branching points
150
100
50
0
**
Sibling
pdgfrb uq30bh
d
Large vessel diameter (µm)
100
80
60
40
20
0
**
Capillary diameter (µm)
8
6
4
2
0
ns
Sibling
pdgfrb uq30bh
e
2000 kDa Dextran
70 kDa Dextran
e′
70 kDa Dextran
Sibling
pdgfrb uq30bh
f
Normal
Mild
Severe
Aneurysm phenotype (%)
100
50
0
Sibling
pdgfrb uq30bh
g
Dextran intensity
0.6
0.4
0.2
0.0
ns
Sibling
pdgfrb uq30bh

Extended Data Figure 2

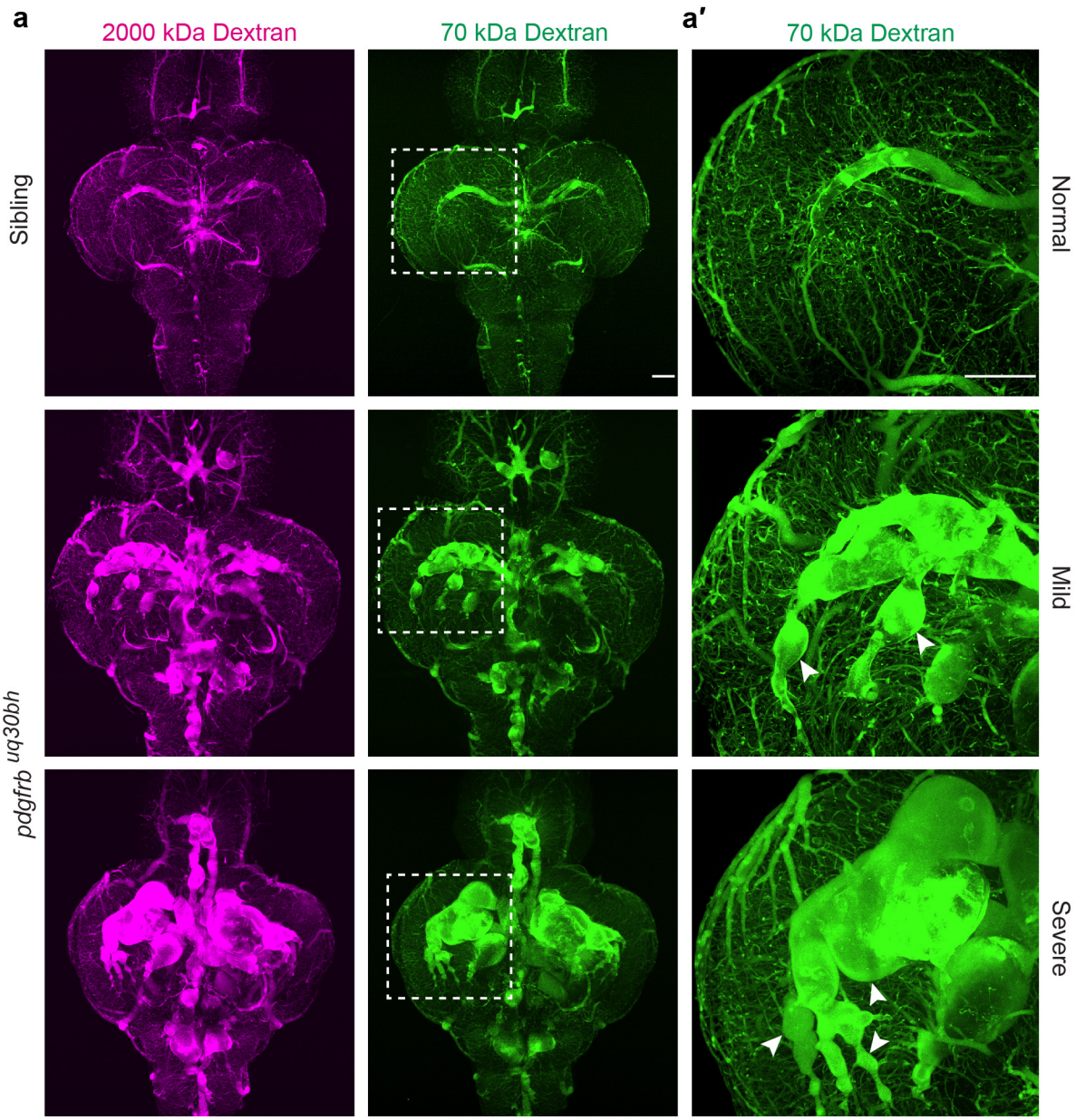

Figure 3

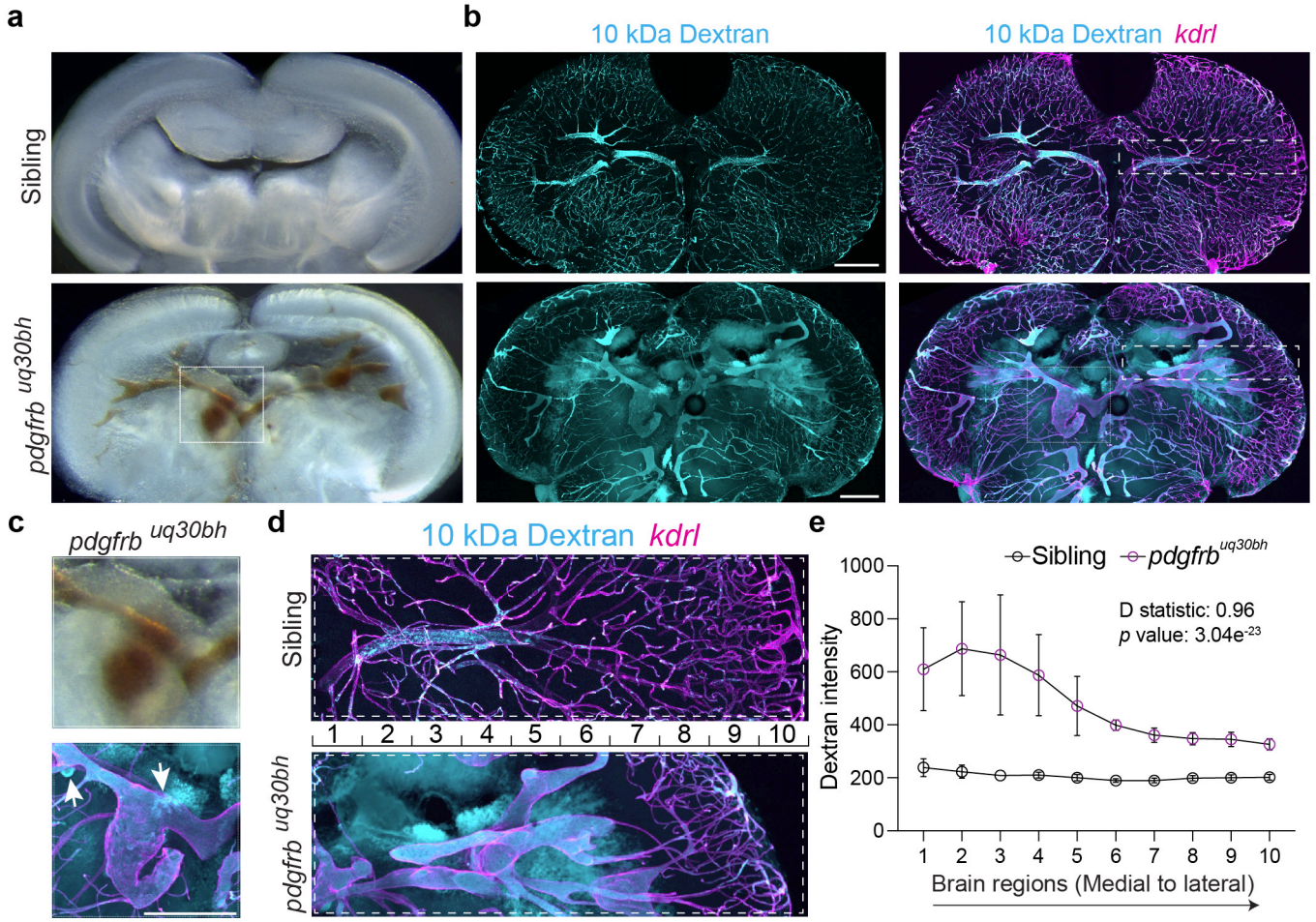
a
b
10 kDa Dextran
10 kDa Dextran kdrl
Sibling
pdgfrb uq30bh
c
pdgfrb uq30bh
d
10 kDa Dextran kdrl
Sibling
pdgfrb uq30bh
1 2 3 4 5 6 7 8 9 10
e
Sibling
pdgfrb uq30bh
D statistic: 0.96
p value: 3.04e-23
Dextran intensity
1000
800
600
400
200
0
1 2 3 4 5 6 7 8 9 10
Brain regions (Medial to lateral)

Extended Data Figure 3

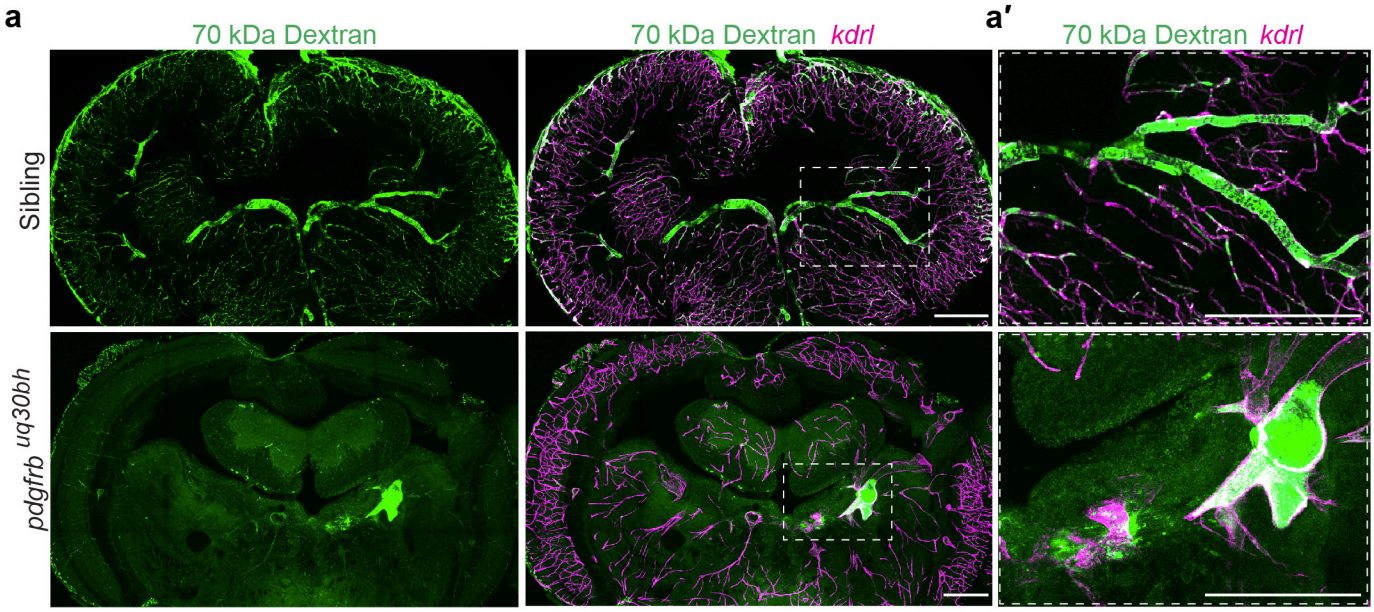

Figure 4

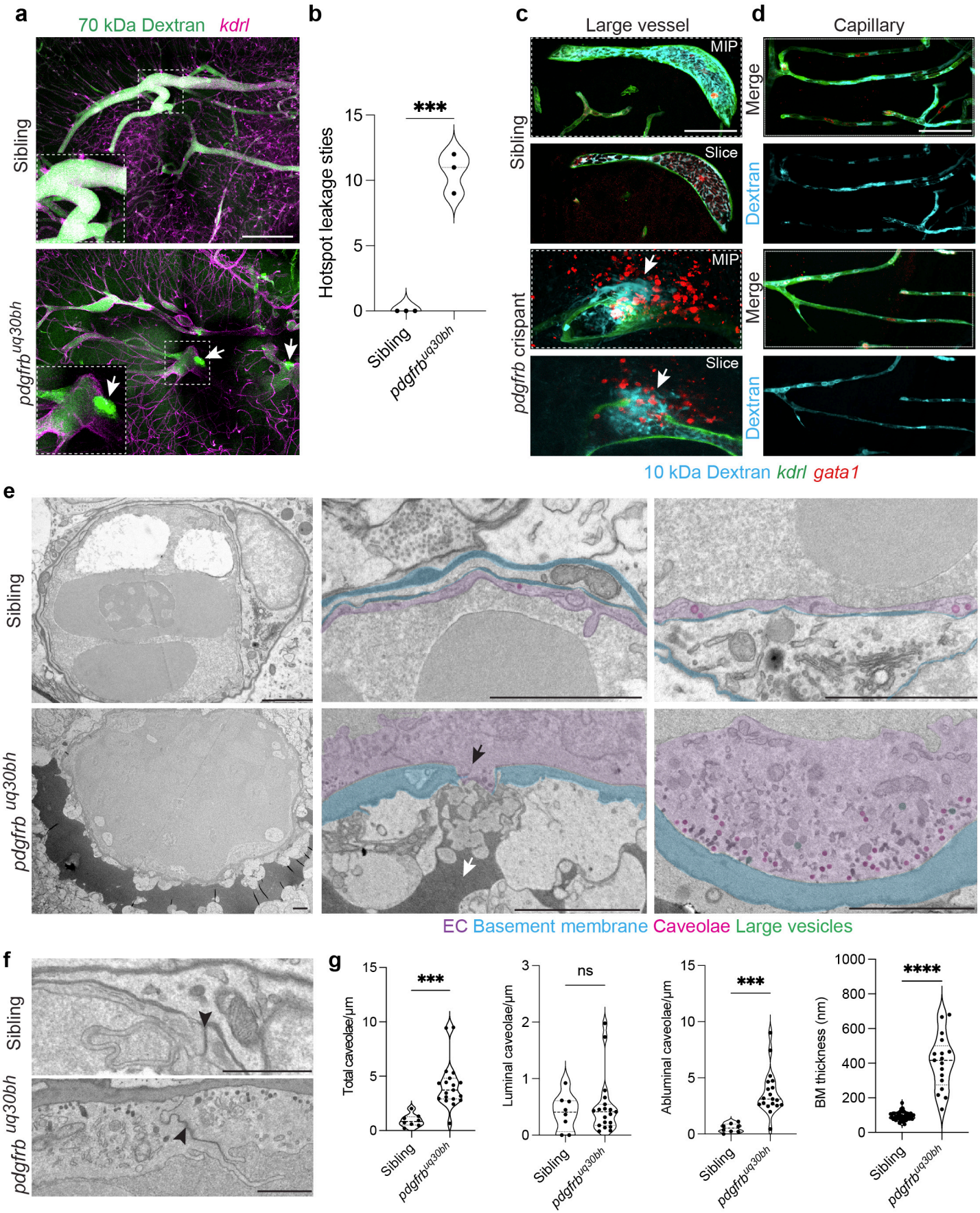
a
70 kDa Dextran kdrl
Sibling
pdgfrb uq30bh
b
Hotspot leakage sties
***
Sibling
pdgfrb uq30bh
c
Large vessel
MIP
Slice
Sibling
pdgfrb crispant
d
Capillary
Merge
Dextran
10 kDa Dextran kdrl gata1
e
Sibling
pdgfrb uq30bh
EC Basement membrane Caveolae Large vesicles
f
Sibling
pdgfrb uq30bh
g
Total caveolae/µm
***
Luminal caveolae/µm
ns
Abluminal caveolae/µm
***
BM thickness (nm)
****
Sibling
pdgfrb uq30bh

Extended Data Figure 4

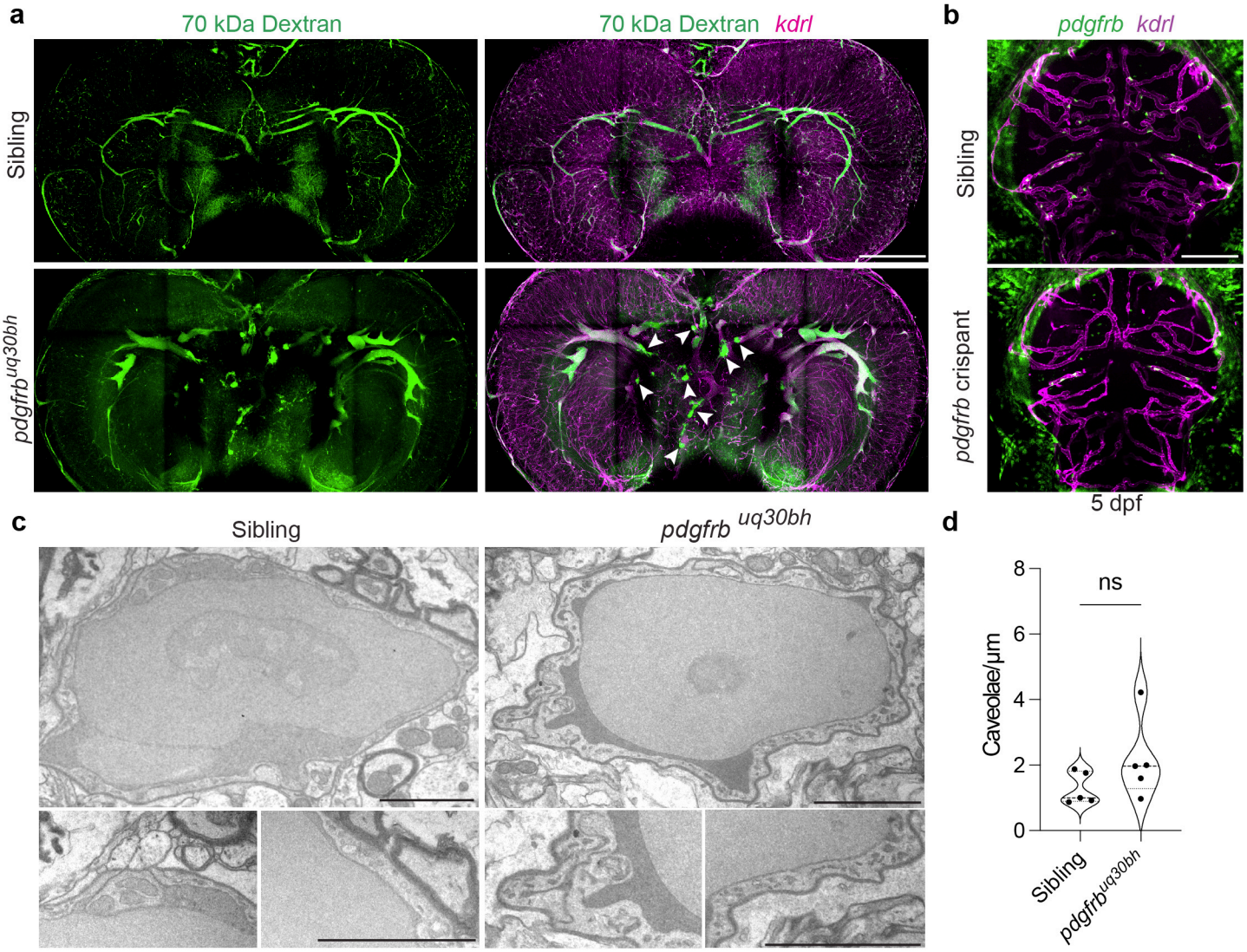

Supplementary materials

Vascular mural cells protect the adult brain from haemorrhage but do not control the blood-brain barrier in developing zebrafish

Oguzhan F Baltaci[1,2], Andrea Usseglio Gaudi[1,2], Stefanie Dudczig[1,2], Weili Wang[3], Maria Cristina Rondon-Galeano[1,2], Ye-Wheen Lim[3], James Rae[3], Anne Lagendijk[3], Robert G Parton[3,6], Alison Farley[1,2,4], Benjamin M Hogan[1,2,5,#]

[1] Organogenesis and Cancer Program, Peter MacCallum Cancer Centre, Melbourne, VIC 3000, Australia.
[2] Sir Peter MacCallum Department of Oncology, University of Melbourne, Melbourne, VIC 3000, Australia.
[3] Institute for Molecular Bioscience, The University of Queensland, St Lucia, 4072, QLD, Australia
[4] Walter and Eliza Hall Institute of Medical Research, Melbourne, Victoria 3052, Australia.
[5] Department of Anatomy and Physiology, University of Melbourne, Melbourne, VIC 3000, Australia.
[6] Centre for Microscopy and Microanalysis, The University of Queensland, St Lucia, 4072, QLD, Australia

[#] *Author for Correspondence:*

Professor Ben Hogan
Organogenesis and Cancer Program,
Peter MacCallum Cancer Centre,
Melbourne, VIC 3000, Australia
E-mail: ben.hogan@petermac.org

Zebrafish husbandry

Zebrafish work was conducted in compliance with animal ethics committees at the Peter MacCallum Cancer Centre, The University of Melbourne and The University of Queensland. Previously published transgenic lines were

TgBAC(pdgfrb:egfp)^{ncv22} [1], *Tg(kdrl:Hsa.HRAS-mCherry)*^{s843} [2], *Tg(kdrl:EGFP)*^{s843} [3] and *Tg(gata1:DsRed)*^{sd2} [4].

Genome editing and genotyping

The *pdgfrb*^{uq30bh} mutant strain was generated using CRISPR/Cas9-mediated genome editing. The resulting allele carries a 39-bp deletion and a 5-bp insertion in exon 3 of *pdgfrb* (ENSDARG00000100897), causing a frameshift and premature stop codon.

The gRNA sequence and genotyping primers used were:

gRNA binding site: 5′ GATGGTGACTAAGACGCGA 3′
Forward genotyping primer: 5′ CTTCCTTAGATCCTGACGTGTG 3′
Reverse genotyping primer: 5′ TATTGATGGGTTCGTCACCAG 3′

The *pdgfrb* F0 crispants used were generated as F0 Animals by CRISPR/Cas9-mediated genome editing using predesigned Alt-R CRISPR-Cas9 gRNAs (IDT). The gRNA sequence and genotyping primers used were:

Dr.Cas9.PDGFRB.1.AA: 5′ GATGGTGACTAAGACGCGAG 3′
Forward genotyping primer: 5′ CTTCCTTAGATCCTGACGTGTG 3′
Reverse genotyping primer: 5′ TATTGATGGGTTCGTCACCAG 3′
Dr.Cas9.PDGFRB.1.AB: 5′ CTCGGTGCACACATAAACCC 3′
Forward genotyping primer: 5′ GACGAGAACATCCCAGACTTTC 3′
Reverse genotyping primer: 5′ GCGTGTAAACAAATCCTAACGG 3′

Tracer dye injections and imaging

For all injections at larva and juvenile stages, NHS Ester–Alexa Fluor 405 (Thermo Fisher: A30000) or 10 kDa Dextran–Cascade Blue (Thermo Fisher: D1976) or 70 kDa Dextran–Fluorescein (Thermo Fisher: D1822) were mixed and co-injected with 2000 kDa Dextran–Tetramethylrhodamine (Thermo Fisher: D7139). This allowed for the normalisation of dye signal relative to the larger molecular weight 2000 kDa tracer to ensure that the amount injected intravenously was appropriately controlled for in all imaging experiments. A final concentration of 5 mg/ml for each tracer was used in all injections.

7 dpf larvae were anesthetised with tricaine and mounted laterally with 0.5% low-melting point agarose (Bio-Rad, 1613112) in E3 embryo water on a 35-mm glass bottom dish (MatTek: P35G-1.5-20-C). 5nl of the tracer mix was injected into the posterior cardinal vein (PCV) and larvae were recovered from agarose using a glass pipette into E3 embryo water. 14 dpf larvae were anesthetised with tricaine, placed laterally on a 3% agarose injection mold. 10 nl tracer mix was injected into the PCV and larvae were recovered in E3 embryo water.

For live imaging, larvae were mounted ventrally with 0.5% low-melting point agarose in E3 embryo water on a 35-mm glass bottom dish. All larvae were carefully live imaged at 2 hours

post injection, with a maximum variation in timing of 15 minutes due to the sequential imaging, using Nikon TiE with Yokogawa CSU-W1 spinning disk with Andor Sona sCMOS camera, 40X 1.15 NA water immersion objective for 7 dpf larvae and 20X 0.75 NA objective for 14 dpf (1 um z-step for each stage).

Injections at juvenile and adult stages were performed retro-orbitally using a glass capillary needle as previously described[5]. For juvenile stage (2-month post fertilisation), brains were extracted 2 hours post injection and whole brains were tissue-cleared using the CUBIC-based method previously described[6]. Briefly, brains were fixed in 2% paraformaldehyde (PFA) at 4°C overnight, washed in PBS, incubated in CUBIC-L solution at 37°C overnight, washed and incubated in PBS at 4°C overnight, then incubated in CUBIC-R solution at room temperature overnight. Brains were mounted ventrally with 2% agarose in CUBIC-R on a 35-mm glass bottom dish and imaged using Nikon TiE with Yokogawa CSU-W1 spinning disk with Andor Sona sCMOS camera, 4X 0.2 NA objective, 10X 0.45 NA objective, and 20X 0.75 NA objective. For adult stage (>2.5-months post fertilisation), Cascade Blue 10- or 70 kDa Dextran were injected as previously described[5]. Brains were extracted 2 hours post injection, fixed in 2% PFA overnight, washed in PBS. For vibratome sectioning, brains were embedded in 7% low-melting agarose in PBS in cryomolds (Tissue-Tek) and were sectioned coronally using a vibrating microtome (Leica VT1000 S) with 200 µm thickness setting. Selected sections were placed on a microscope slide and were incubated with RapiClear 1.52 solution (SunJin Lab, RC152201) for 3 hours at room temperature. Imaging was performed using Olympus FV3000 confocal microscope with 10X 0.4 NA objective with 5 µm step size and 40X 1.4 NA oil immersion objective with 1 µm step size. For whole brain imaging, brains were tissue cleared as described earlier and were imaged using Olympus FV3000 confocal microscope with 10X 0.4 NA objective with 5 µm step size. Videos highlighting the “hotspot” leakage sites were generated using Imaris 10.1 software (Bitplane) and Adobe Premier Pro 2024.

Live imaging of pericytes and blood vessels was conducted using Olympus FV-MPERS multiphoton microscope with 25X 1.05 NA water dipping objective with 3 µm step size. To ensure optical transparency, live imaging was conducted in F0 knockout animals for the gene *slc45a2* (ENSDARG00000002593) as previously described[7] or 0.003% PTU was applied to the embryo water at 1 dpf.

Transmission electron microscopy

Brains were extracted from euthanised 5-month-old zebrafish, fixed in 2.5% glutaraldehyde for 1 hour at room temperature and washed with PBS. For sectioning, the brains were embedded in 7% low-melting point agarose in PBS in cryomolds (Tissue-Tek) and were sectioned coronally using a vibrating microtome (Leica VT1000 S) with 200 µm thickness. Tissue sections were processed as described previously[8].

Briefly, tissue sections were immersed consecutively in a series of aqueous solutions: 1.5% potassium ferricyanide and 2% osmium tetroxide, 1% thiocarbohydrazide, 2% osmium tetroxide, 2% uranyl acetate and 0.06% lead nitrate using a Pelco Biowave at 80W under vacuum for 3min each. Vibratome sections then underwent serial dehydration in increasing concentrations of ethanol, before serial infiltration with increasing concentrations of Procure 812 resin. Ultrathin sections were obtained using a Leica UC64 ultramicrotome and imaged on a Jeol JEM-1011 at 80kV.

Quantifications

Vessel length, diameter and branching points

Vessel length, diameter and branching points were quantified using Imaris 10.1 software (Bitplane). For larval stages, lumenized midbrain central artery (*kdrl:Hsa.HRAS-mCherry)* branching from the middle mesencephalic arteries was traced using the filament tool and the total filament length (µm) was plotted. The branching points within the traced blood vessels were quantified by manual scoring in 3D view. For adult stage, 100-µm thick maximum intensity projections (MIP) were generated from whole brain imaging, using the continuation of the left middle mesencephalic central artery as an anatomical anchor point as the consistent region measured. For diameter measurements, 10 capillary diameters were measured per sample. Vessel anatomy was identified using the study by Isogai et al[9] as a reference.

Tracer intensity

Tracer intensity quantification was performed on genotype blinded image sets using Fiji[10]. For larval stage experiments, the tracer accumulation in brain parenchyma (70-or 10 kDa Dextran or 1 kDa NHS Ester) was calculated using average intensity from 4 midbrain parenchymal regions in 50-µm thick MIPs, which were generated starting from 50 µm below dorsal longitudinal vessel (DLV) to avoid detecting potential leakage from surface vessels. These measurements were normalized to the vascular tracer intensity of 2000 kDa Dextran, which was calculated using average intensity from 4 regions within the DLV lumen. As such, for each data point: intensity=parenchymal dextran (1, 10 or 70 kDa) intensity/luminal 2000 kDa Dextran intensity.

For juvenile stage experiments, 30-µm thick MIPs were generated starting from 60 µm below the most superficial vessel to potential leakage from the surface vessels. Brain parenchymal 70 kDa Dextran intensity was calculated using average intensity from 4 midbrain parenchymal regions and was normalized to vascular 2000 kDa Dextran intensity, which was calculated using average intensity from 4 regions within the lumen of superficial large calibre vessels. For adult stage experiments, 50-µm thick MIPs were generated and dextran intensity outside the vessels was measured at every 100 µm from medial to lateral direction within 1 mm. Branching point of left and right middle mesencephalic arteries was determined as the starting point.

TEM quantification

Imaged sections were quantified using Fiji[10]. Caveolae were defined as circular profiles of less than 100 nm in diameter and were scored as luminal or abluminal based on proximity to each surface membrane (within 500 µm of each surface or in a thin walled vessel the caveolae closest to each surface). Basement membrane thickness was scored in 6 different locations per vessel that were selected at random. N=3-8 vessels per group were analysed as indicated in the Figure legends.

Statistical analysis

Statistical analyses and graphical representations were conducted using GraphPad Prism 10 software. ns: $P>0.05$, *$P\leq0.05$, **$P\leq0.01$, ***$P\leq0.001$, ****$P\leq0.0001$. For Figure 3e, we applied the non-parametric two-sample Kolmogorov-Smirnov test using Python software to evaluate

whether the distribution of tracer accumulation for each position differed from that of the control. Further details on statistics can be found in each figure legend.

References

1 Ando, K. *et al*. Clarification of mural cell coverage of vascular endothelial cells by live imaging of zebrafish. *Development* **143**, 1328-1339 (2016). https://doi.org:10.1242/dev.132654

2 Chi, N. C. *et al*. Foxn4 directly regulates tbx2b expression and atrioventricular canal formation. *Genes Dev* **22**, 734-739 (2008). https://doi.org:10.1101/gad.1629408

3 Jin, S. W., Beis, D., Mitchell, T., Chen, J. N. & Stainier, D. Y. Cellular and molecular analyses of vascular tube and lumen formation in zebrafish. *Development* **132**, 5199-5209 (2005). https://doi.org:10.1242/dev.02087

4 Traver, D. *et al*. Transplantation and in vivo imaging of multilineage engraftment in zebrafish bloodless mutants. *Nat Immunol* **4**, 1238-1246 (2003). https://doi.org:10.1038/ni1007

5 Pugach, E. K., Li, P., White, R. & Zon, L. Retro-orbital injection in adult zebrafish. *J Vis Exp* (2009). https://doi.org:10.3791/1645

6 Matsumoto, K. *et al*. Advanced CUBIC tissue clearing for whole-organ cell profiling. *Nat Protoc* **14**, 3506-3537 (2019). https://doi.org:10.1038/s41596-019-0240-9

7 Davis, A. E., Castranova, D. & Weinstein, B. M. Rapid Generation of Pigment Free, Immobile Zebrafish Embryos and Larvae in Any Genetic Background Using CRISPR-Cas9 dgRNPs. *Zebrafish* **18**, 235-242 (2021). https://doi.org:10.1089/zeb.2021.0011

8 Lim, Y. W. *et al*. Caveolae Protect Notochord Cells against Catastrophic Mechanical Failure during Development. *Curr Biol* **27**, 1968-1981 e1967 (2017). https://doi.org:10.1016/j.cub.2017.05.067

9 Isogai, S., Horiguchi, M. & Weinstein, B. M. The vascular anatomy of the developing zebrafish: an atlas of embryonic and early larval development. *Dev Biol* **230**, 278-301 (2001). https://doi.org:10.1006/dbio.2000.9995

10 Schindelin, J. *et al*. Fiji: an open-source platform for biological-image analysis. *Nat Methods* **9**, 676-682 (2012). https://doi.org:10.1038/nmeth.2019